Advances in Environmental Research, *Vol. 5, No. 4 (2016) 225-235*
DOI: https://doi.org/10.12989/aer.2016.5.4.225

Enhancement of Methylene Blue dye adsorption by Fe-Hydroxyapatite composite

Deniz İzlen Çifçi*

Çorlu Engineering Faculty, Environmental Engineering Department, Namık Kemal University, No:13 59860 Çorlu / TEKİRDAĞ, Turkey

(Received October 4, 2016, Revised December 6, 2016, Accepted December 6, 2016)

Abstract. Synthesized hydroxyapatite (Hyd) and Fe-hydroxyapatite (Fe-Hyd) composite were used for the removal of Methylene Blue (MB) from aqueous solutions in this study. The effect of adsorbent amount, pH and initial MB concentration were carried out to investigate in the aqueous solution. The kinetic study shows that the MB adsorption process with Hyd or Fe-Hyd follow pseudo-second order kinetic model. Experimental results are well fitted to the Langmuir isotherm model. The maximum adsorption capacities of Hyd and Fe-Hyd were obtained as 2.90 mg/g and 5.64 mg/g for MB according to Langmuir Isotherm models, respectively. Fe-Hyd composite increased the adsorption capacity of Hyd by 1.95 times that Hyd. It is concluded that Fe-Hyd composite is promising and economical adsorbent for MB removal in the aqueous solution.

Keywords: adsorption; composite; dye; hydroxyapatite; synthesis

1. Introduction

Among the many treatment methods used for dyes and heavy metals removal from wastewater, adsorption process is one of the efficient, economic and simple methods (Nguyen and Pho, 2014). Activated carbon is common adsorbent material, but the main disadvantage of it is the high cost (Mahmud *et al*. 2012, Wei *et al*. 2010). Low cost materials have come to gain adsorption process due to the decreasing operational cost.

Hydroxyapatite [$Ca_{10}(PO_4)_6(OH)_2$, (Hyd)] is an inorganic component, commonly used the applications of drug delivery systems, bone grafts and the hard tissues of humans (Zhuang *et al*. 2015, Nie *et al*. 2012). Also, it has been commonly used for different dyes and heavy metals adsorption due to the high specific surface area, low water solubility and stability leading to increase the adsorption capacity (Wei *et al*. 2010, Yang *et al*. 2016). Furthermore, it is environmental friendly and has low-cost and abundant hydroxyl groups (Cui *et al*. 2014). There have been many researches on the removal of heavy metals and dyes using hydroxpatite or modified hydroxyapatite (Mahmud *et al*. 2012, Allam *et al*. 2016, Zhuang *et al*. 2015, Valizadeh *et al*. 2016).

The aim of this study is to investigate MB removal using hydroxyapatite (Hyd) and enhance the

*Corresponding author, Ph.D., E-mail: dicifci@nku.edu.tr

Copyright © 2016 Techno-Press, Ltd.
http://www.techno-press.org/?journal=aer&subpage=7 ISSN: 2234-1722 (Print), 2234-1730 (Online)

removal efficiency by Fe doped hydroxyapatite (Fe-Hyd) and evaluate according to isotherm and kinetic models. For these purposes, Hyd and Fe-Hyd have been employed in aqueous solution containing MB. The adsorbent dosage, pH and initial dye concentration investigated to evaluate in the effect of MB removal.

2. Materials and methods

2.1 Materials

$(NH_4)_2HPO_4$ (≥99.0%, Cat No: 101207), $CaCl_3$ (≥98.0%, Cat No: 102378), NH_3 (25%, Cat No: 1.05422), $FeSO_4.6H_2O$ (≥99.0%, Cat No: 103965), $FeCl_3.6H_2O$ (≥99.0%, Cat No: 103943), HCl (37%, Cat No: 100314), HNO_3 (≥65%, Cat No: 100456) and NaOH (≥99.0%, Cat No: 106462) were purchased from Merck. Distilled water was used to daily prepare all the aqueous solutions.

2.2 Synthesis of composite

Hydroxyapatite and Fe-Hydroxyapatite composites are prepared to use in this experiments.

2.2.1 Preparation of hydroxyapatite composite (Hyd)

Typically, $(NH_4)_2HPO_4$ solution was added to $CaCl_3$ solution slowly with a Ca/P molar ratio of 1.67 at room temperature. The solution pH was adjusted at 10 using NH_3 solution. The solution was ultrasonicated at 10 min and heated at 70°C for 1 hour. The solution was stirred for 24 hours at room temperature to obtain complete precipitation. After 24 hours aging, precipitation was rinsed by distilled water several times to remove NaCl from precipitation. Precipitation dried 105°C for 24 h.

2.2.2. Preparation of Fe-Hydroxyapatite composite (Fe-Hyd)

Typically, $(NH_4)_2HPO_4$ solution was added to $CaCl_3$ solution slowly with a Ca/P molar ratio of 1.67 at room temperature. $FeSO_4.6H_2O$ and $FeCl_3.6H_2O$ was dissolved in 200 mL distilled water with the molar ratio of Fe^{3+} to Fe^{2+} to be 2:1 in the solution and iron weight ratio of 5% according to total weight of $Ca_{10}(PO_4)_6(OH)_2$. Two solutions were mixed and the pH was adjusted at 10 using NH_3 solution. The solution was ultrasonicated at 10 min and heated at 70°C for 1 hour. The solution was stirred for 24 hours at room temperature to obtain complete precipitation. After 24 hours aging, precipitation was rinsed by distilled water several times to remove NaCl from precipitation. Precipitation dried 105°C for 24 h.

2.3 Adsorption experiments

Adsorption experiments were performed using 100 mL volume, 150 rpm shaking speed, 25°C constant temperature and adsorption time was selected 24 hours. 500 mg/L of MB solution are prepared using distilled water as a stock solution. The pH was adjusted to the desired levels using HNO_3 (1 N) and NaOH (1 N). Taken samples were centrifuged at 4000 rpm for 5 min before analysis. Composite concentrations, pH and dye concentration were varied at the ranges of 0.25-2.0 g, 3-11 and 10-100 mg/L, respectively. 50 mg/L MB was used a range of 0.25-2.0 g composite at pH 7 to investigate the effect of composite amount, 50 mg/L MB was used a pH range of 3-11 at

0.75 g of composite to determine the effect of pH and 0.75 g composite was used a MB concentration of 10-100 mg/L at pH 9 to evaluate the effect of initial MB concentration.

2.4 Analysis

The pH was measured using a pH meter (WTW pH 315i). Synthesized Hyd and Fe-Hyd composites were characterized using electron scanning microscopy (SEM)-energy dispersive X-ray analyzer (EDX) (FEI-QUANTA FEG 250) to obtain information about surface properties and chemical characterization of composites. SEM conditions follow: spot 3.5, HV 2 kV, pressure 50 Pa, detector LFD. The pH_{pzc} (pH point of zero charge) of the samples was determined from the literature (Asgari *et al*. 2013). The concentration of Methylene Blue (MB) was analyzed using UV spectrophotometer (Shimadzu UV-2401 PC instrument) at maximum wavelength (664 nm).

2.5 Adsorption kinetic and isotherm models

Adsorption kinetic constants were calculated at the conditions of 50 mg/L MB, pH=9 and Hyd or Fe-Hyd amounts 0.75 g and the four different kinetics formulas are given in Table 1. In the adsorption isotherm studies, the Hyd or Fe-Hyd (1 g) added into solutions at ranging initial MB concentrations from 10 to 100 mg/L. Later, a series of isotherm models of Langmuir, Freundlich, Temkin and Dubinin-Radushkevich (D-R) were applied to data sets to calculate according to Table 2.

Error function assessment was used to compare Isotherm models and experimental results. Four error functions namely average relative error (AER), sum square error (EERSQ), sum of absolute error (EABS) and hybrid fractional error function (HYBRID) were calculated according to given in Table 3.

Table 1 Equations of kinetics

Kinetic Models	Linear Equations	Reference
Pseudo first order	$\ln(q_e - q_t) = \ln q_e - k_1 t$	Saber-Samandari *et al.* (2014)
Pseudo second order	$\frac{t}{q_t} = \frac{1}{k_2 q_e^2} + \frac{t}{q_e}$	Saber-Samandari *et al.* (2014)
Elowich	$q_t = \frac{1}{\beta}\ln \alpha\beta + \frac{1}{\beta}\ln t$	Saber-Samandari *et al.* (2014)
Intraparticle diffusion	$q_{t=k_i} t^{0.5} + C_i$	Saber-Samandari *et al.* (2014)

Table 2 Equations of isotherm models

Isotherm Models	Linear Equations	Reference
Langmuir	$\frac{C_e}{q_e} = \frac{1}{k_L q_m} + \frac{C_e}{q_m}$	Moreno-Piraján *et al.* (2011)
Freundlich	$log q_e = log K_F + \frac{1}{n} log C_e$	Moreno-Piraján *et al.* (2011)
Temkin	$q_e = B.lnA + B.lnC_e$	Dawodu *et al.* (2014)
Dubinin-Radushkevich	$lnq_e = lnq_m - \beta\varepsilon^2$	Dawodu *et al.* (2014)

Table 3 Equations of error functions

Error Functions	Equations	Reference
ARE	$\frac{100}{n}\sum_{i=1}^{n}\left\|\frac{q_{e,m}-q_{e,c}}{q_{e,m}}\right\|$	Hashem *et al.* (2016)
ERRSQ	$\sum_{i=1}^{n}\left(\left(q_{e,c}-q_{e,m}\right)^2\right)$	Hashem *et al.* (2016)
EABS	$\sum_{i=1}^{n}\left\|q_{e,m}-q_{e,c}\right\|$	Sarici Özdemir and Önal (2014)
HYBRID	$\frac{100}{n-p}\sum_{i=1}^{n}\frac{(q_{e,m}-q_{e,c})^2}{q_{e,m}}$	Sarici Özdemir and Önal (2014)

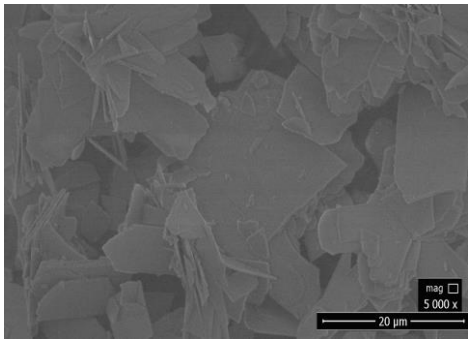

Fig. 1 SEM image of Hyd composite

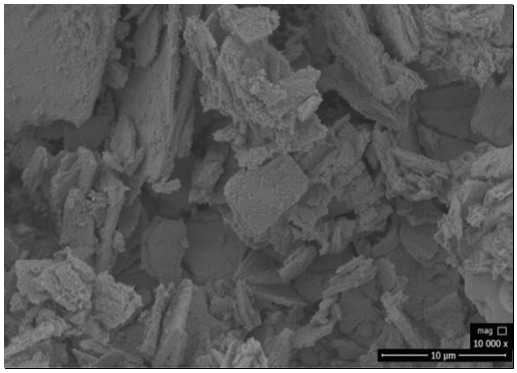

(a) 10000× zoom

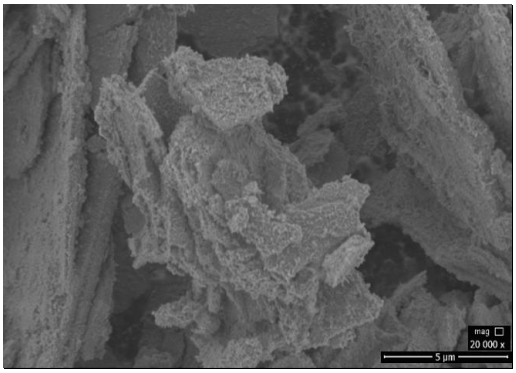

(b) 20000× zoom

Fig. 2 SEM images of Fe-Hyd composite

3. Results and discussion

3.1 SEM-EDX analysis of composites

SEM analysis of Hyd and Fe-Hyd are given Figs. 1-2. Hydroxypatite has irregular shapes and

the surface is smooth. On the contrary, the surface of Fe-Hyd is rough due to the iron nanoparticles on the surface as seen in SEM images. Similar crystalline shapes observed in the literature (Valizadeh *et al.* 2016). According to EDX spectrum results that Hyd is mainly composed of calcium, phosphorus and oxygen as in the literature (Feng *et al.* 2010). Hyd composite contains 69.1% O, 15.8% P, 0.6% Cl, 14.4% Ca and Fe is not observed while Fe ratio is 2.0% in the Fe-Hyd composite.

3.2 Effect of composite amounts

The effect of Hyd or Fe-Hyd composite amount was investigated on the removal of MB (Fig. 3). MB removal increased with enhancing the composite amount both of the composites due to the increase of the available adsorption sites (Wei *et al.* 2010). Above 1 g of Fe-Hyd, MB removal became very slow but it continued to increase with Hyd composite. MB removal was obtained as 11.3% and 63.5% by using hydroxyapatite. MB removal increased from 20.2% to 78.6% when Fe-Hyd enhanced from 0.25 to 2.0 g composite, respectively. However, the adsorption capacity dramatically decreased from 2.25 to 1.80 mg/g using Hyd composite and decreased from 4.30 to 3.71 mg/g using Fe-Hyd composite when the composite amount increased from 0.75 to 1.0 g due to the adding excess surface area of composite. Furthermore, MB removal increased 2.08 times when 2% of iron nanoparticles doped on the surface of hydroxyapatite.

3.3 Effect of pH

MB removal changes in different pH values is given in Fig. 4. It can be seen that MB adsorption increased as the pH increased and adsorption of MB enhanced the alkaline conditions by using Hyd or Fe-Hyd. The effect of pH on adsorption depends on the point zero charge (pH_{pzc}) of adsorbent and the degree of ionization of the pollutant (Ai *et al.* 2011). The value of pH_{pzc} was found to be 7.59 and 7.82 by Hyd and Fe-Hyd, respectively. These result similar in the literature that the pH_{pzc} of hydroxyapatite was found to between 7.6 and 8.6 (Bell *et al.* 1973). This means that when the solution of $pH<pH_{pzc}$, the surface of hydroxyapatite is positively charged and this leads to decrease the adsorption of the cationic dyes. As known, MB is the cationic dye and higher

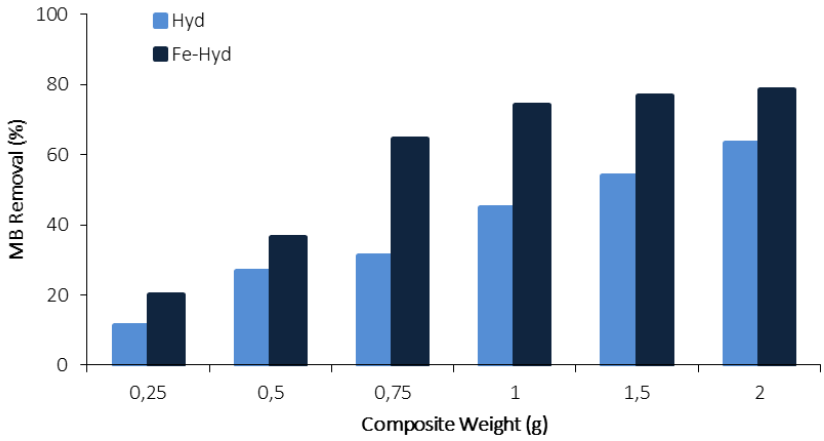

Fig. 3 MB removal changes on different composite concentrations (MB: 50 mg/L, pH 7, 24 h)

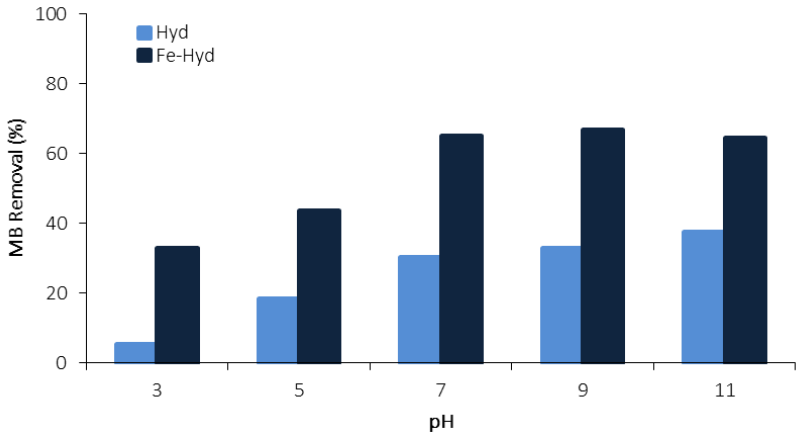

Fig. 4 MB removal changes on different pH (MB: 50 mg/L, composite: 0.75 g, 24 h)

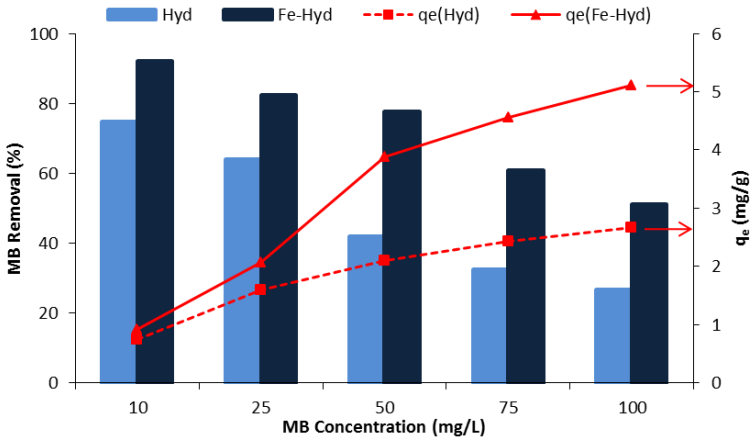

Fig. 5 MB removal changes on different initial MB concentration (Composite: 0.75 g, pH: 9, 24 h)

adsorption of MB can be favored above the pH_{pzc} of hydroxyapatite (Allam *et al.* 2016). MB adsorption increased from 5.30 to 37.69% and from 33.01% and 64.51% with the increasing the pH from 3.0 to 11 by using Hyd and Fe-Hyd, respectively.

3.4 Effect of initial dye concentration

MB removal decreased with increasing initial MB concentration in both composites due to the saturation of the Hyd and Fe-Hyd surface (Fig. 5). Particularly, MB adsorption efficiencies were 74.7% and 92.1% at 10 mg/L MB concentration and it decreased to 26.6% and 51.2% at 100 mg/L MB concentrations by using Hyd and Fe-Hyd, respectively. It can be clearly seen that the adsorption capacity increases all concentrations by using Fe-Hyd composite. It is observed that the MB adsorption capacity was 1.2-1.9 higher by using Fe-Hyd than Hyd composite at varying initial MB concentrations. Although MB removal decreased with increasing initial MB concentration, MB adsorption capacities increased with increasing initial MB concentration. When the initial MB

concentration increased from 10 mg/L to 100 mg/L, the adsorption capacity increased from 0.9 to 5.1 mg/g while it enhanced from 0.7 to 2.7 mg/g using 0.75 g Hyd or Fe-Hyd composites. This could be explained that increasing of initial MB concentration supplies the enhancing of driving force to overcome the mass transfer resistances of the pollutant between the liquids and hydroxyapatite composites (Low *et al.* 2013).

3.5 Evaluation kinetics

Although the values of R^2 is greater than 0.9 in all the kinetic models, the linear fitting results show that the pseudo-second-order kinetic model gave the best fit according to R^2 (0.99) from Table 4. This could be explained that the rate limiting step of MB adsorption by using Fe-Hyd might be chemisorption between Fe-Hyd and MB. The pseudo second order kinetic rates of Hyd and Fe-Hyd were found 0.032 and 0.146 g/mg.h, respectively. Srilakshmi and Saraf (2016) founded that pseudo-second-order kinetic model provides the best correlation than the other kinetic models for Congo Red dye adsorption using hydroxyapatite and Ag doped hydroxyapatite. Besides, adsorption of Direct Red 23 using hydroxyapatite is fitted pseudo-second-order kinetic model (Valizadeh *et al.* 2016). Elovich and Intraparticle diffusion kinetic gave lowest values of R^2 that these kinetics are not suitable for the adsorption of MB using Hyd or Fe-Hyd.

3.6 Evaluation isotherms models

The Langmuir, Freundlich, Temkin and Dubinin-Radushkevich isotherm models applied in this study and Langmuir, Freundlich, Temkin and Dubinin-Radushkevich Isotherms parameters for Hyd and Fe-Hyd are given in Table 5. The regression coefficients of both Hyd and Fe-Hyd at Langmuir Isotherm are greater than that other Isotherm models, indicating that the Langmuir model fit the experimental well and both of the composite adsorption demonstrated the monolayer adsorption on the active site of the surface (Nie *et al.* 2012).

Furthermore, the lowest error function values were observed with Langmiur Isotherm followed by Temkin Isotherm indicating a better fit than the other models using Fe-Hyd composites while error values of Temkin Isotherm Model are lower than the Freundlich Isotherm Model using Hyd composite. The highest error values are obtained the Dubinin-Radushkevich Isotherm Model

Table 4 Kinetic constants values of Hyd and Fe-Hyd

Kinetic Model	Parameters	Units	Hyd	Fe-Hyd
Pseudo first order	k_1	h^{-1}	0.201	0.329
	R^2	-	0.9360	0.9579
Pseudo second order	k_2	g/(mg.h)	0.032	0.146
	R^2	-	0.9950	0.9905
Elovich	A	g/mg	2.43	2.60
	B	mg/(g.h)	1.71	0.84
	R^2	-	0.9086	0.9438
Intraparticle diffusion	k_i	$mg/(g.h^{0.5})$	0.510	0.989
	R^2	-	0.9072	0.9273

Table 5 Adsorption isotherm model parameters by Hyd and Fe-Hyd derived from Langmuir model, Freundlich model, Temkin model, and Dubinin-Radushkevich model

Adsorption Isotherm	Parameters	Units	Hyd	Fe-Hyd
Langmiur	q_{max}	mg/g	2.90	5.64
	K_L	L/mg	0.12	0.18
	R_L		0.08	0.05
	R^2	-	0.9957	0.9947
	ARE		5.7009	10.5824
	ERRSQ		0.0470	0.2541
	EABS		0.4470	0.9938
	HYBRID		0.5703	2.8792
Freundlich	n	-	2.76	2.34
	K_F	mg/g	0.60	1.10
	R^2	-	0.9631	0.9410
	ARE		8.3461	8.9260
	ERRSQ		0.1241	1.1287
	EABS		0.6679	1.6706
	HYBRID		1.4771	5.3031
Temkin	A	L/mg	1.69	2.58
	B		0.55	1.00
	R^2	-	0.9929	0.9687
	ARE		3.3238	10.8413
	ERRSQ		0.0165	0.5801
	EABS		0.2270	1.1341
	HYBRID		0.2349	4.1899
Dubinin-Radushkevich	q_m	mg/g	2.45	4.79
	β	mg^2/J^2	-6.10^{-6}	-3.10^{-6}
	R^2	-	0.9596	0.9798
	ARE		23.4687	21.6569
	ERRSQ		0.6165	1.0975
	EABS		1.2305	1.2392
	HYBRID		14.3749	19.5993

for both Hyd and Fe-Hyd composites. It was shown that Fe-Hyd indicated higher MB adsorption capacity from obtaining Langmuir Isotherm Models. The value of R_L in Langmuir Isotherm should be between 0 and 1 for the good adsorption (Saber-Samandari *et al.* 2014). The R_L is 0.08 and 0.05 for Hyd and Fe-Hyd composite, respectively. This suggests that adsorption is favorable for the uptake of MB both of the composites. The heterogeneity factor which related the bonding between adsorbent and adsorbate, ranged $0<1/n<0.5$ indicated the suitability of adsorption process and it is founded 0.36 and 0.43 for Hyd and Fe-Hyd composite, respectively (Cui *et al.* 2014). Besides, all the isotherm parameters show to improve by Fe impregnated on the surface of hydraxyapatite.

Thus, Fe-Hyd composite could be more suitable and effective adsorbent for removing of MB from aqueous solutions. MB adsorption capacity increased 1.85 times by using Fe-Hyd comparing the Hyd composite. As shown in Table 5, ERRSQ error function are the lowest values when it compares the other error functions.

Comparison of experimental results and isotherm models is given in Figs. 6-7. It is observed that the MB adsorption capacity of Fe-Hyd increases with increasing MB concentration up to equilibrium due to the availability of active sites on Fe-Hyd composite. On the other hand, MB adsorption capacity of Fe-Hyd is more appropriate than Hyd composite. It can be seen that Isotherm Model values are similar and very closed with experimental values. The Freundlich model for Fe-Hyd and the Dubinin-Radushkevich model for Hyd have the lowest the R^2 value when the comparing the other models of R^2 (Table 5).

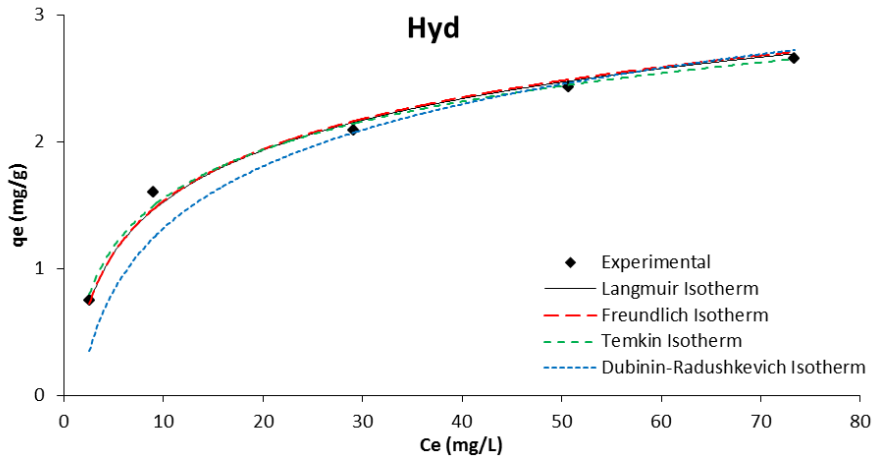

Fig. 6 Comparison experimental results and adsorption isotherms of MB removal using the Hyd composite

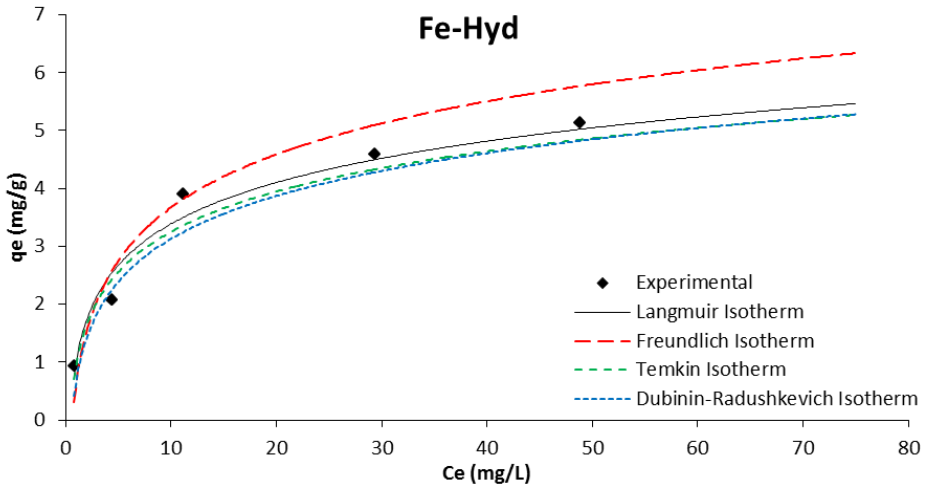

Fig. 7 Comparison experimental results and adsorption isotherms of MB removal using the Fe-Hyd composite

5. Conclusions

It is demonstrated that the hydroxyapatite composite can be efficiently used the MB adsorption and MB adsorption capacity could be increased by using iron magnetite doped hydroxyapatite. Effect of composite amount, pH and initial MB concentration were investigated in this study and the optimum values were determined. The experiments showed that the pseudo-second-order kinetic model and the Langmuir model are the best fitted the experiment results both of Hyd and Fe-Hyd composites. All the experimental results in this study indicate that obtained MB removal using Fe-Hyd composite is higher than the using Hyd composite at all conditions such as pH, initial MB concentration, etc. It was concluded that hydroxyapatite could be promising composite in dye adsorption and enhancing of the adsorption efficiency is provided by iron doping on the surface of hydroxyapatite.

Acknowledgements

This study was financially supported by NKU Research Funding Project (NKUBAP.00.17.AR.14.01).

References

Ai, L., Zhang, C., Liao, F., Wang, Y., Li, M., Meng, L. and Jiang, J. (2011), "Removal of methylene blue from aqueous solution with magnetite loaded multi-wall carbon nanotube: Kinetic, isotherm and mechanism analysis", *J. Hazard. Mater.*, **198**, 282-290.

Allam, K., El Bouari, A., Belhorma, B. and Bih, L. (2016), "Removal of methylene blue from water using hydroxyapatite submitted to microwave irradiation", *J. Water Resource Prot.*, **8**(03), 358-371.

Asgari, G., Mohammadi, A.S., Mortazavi, S.B. and Ramavandi, B. (2013), "Investigation on the pyrolysis of cow bone as a catalyst for ozone aqueous decomposition: Kinetic approach", *J. Anal. Appl. Pyrol*., **99**, 149-154.

Bell, L.C., Posner, A.M. and Quirk, J.P. (1973), "The point of zero charge of hydroxyapatite and fluorapatite in aqueous solutions", *J. Colloid Interf. Sci.*, **42**(2), 250-261.

Cui, L., Hu, L., Guo, X., Zhang, Y., Wang, Y., Wei, Q. and Du, B. (2014), "Kinetic, isotherm and thermodynamic investigations of Cu2+ adsorption onto magnesiumhydroxyapatite/ferroferric oxide nano-composites with easy magnetic separation assistance", *J. Mol. Liq.*, **198**, 157-163.

Dawodu, F.A. and Akpomie, K.G. (2014), "Simultaneous adsorption of Ni(II) and Mn(II) ions from aqueous solution unto a Nigerian kaolinite clay", *J. Mater. Res. Technol.*, **3**(2), 129-141.

Feng, Y., Gong, J.-L., Zeng, G.-M., Niu, Q.-Y., Zhang, H.-Y., Niu, C.-G., Deng, J.-H. and Yan, M. (2010), "Adsorption of Cd (II) and Zn (II) from aqueous solutions using magnetic hydroxyapatite nanoparticles as adsorbents", *Chem. Eng. J.*, **162**(2), 487-494.

Hashem, A., Ahmad, F. and Badawy, S.M. (2016), "Adsorption of direct green 26 onto fix 3500 treated sawdust: equilibrium, kinetic and isotherms", *Desalin. Water Treat.*, **57**(28), 13334-13346.

Low, L.W., Teng, T.T., Rafatullah, M., Morad, N. and Azahari, B. (2013), "Adsorption studies of methylene blue and malachite green from aqueous solutions by pretreated lignocellulosic materials", *Separ. Sci. Technol.*, **48**(11), 1688-1698.

Mahmud, K., Islam, Md. A., Mitsionis, A., Albanis, T. and Vaimakis, T. (2012), "Adsorption of direct yellow 27 from water by poorly crystalline hydroxyapatite prepared via precipitation method", *Desalin. Water Treat.*, **41**(1-3), 170-178.

Nguyen, V.C. and Pho, Q.H. (2014), "Preparation of chitosan coated magnetic hydroxyapatite nanoparticles and application for adsorption of reactive blue 19 and Ni^{2+} ions", *Sci. World J.*, **2014**, ID 273082, 1-9.

Nie, Y., Hu, C. and Kong, C. (2012), "Enhanced fluoride adsorption using Al (III) modified calcium hydroxyapatite", *J. Hazard. Mater.*, **233-234**, 194-199.

Saber-Samandari, S., Nezafati, N. and Kovan, Y. (2014), "Efficient removal of lead (II) ions and methylene blue from aqueous solution using chitosan/Fe-hydroxyapatite nanocomposite beads", *J. Environ. Manage.*, **146**, 481-490.

Sarici-Özdemir, Ç. and Önal, Y. (2014), "Error analaysis studies of dye adsorption onto activated carbon from aqueous solutions", *Particul. Sci. Technol.*, **32**(1), 20-27.

Srilakshmi, C. and Saraf, R. (2016), "Ag-doped hydroxyapatite as efficient adsorbent for removal of Congo red dye from aqueous solution: Synthesis, kinetic and equilibrium adsorption isotherm analysis", *Micropor. Mesopor. Mat.*, **219**, 134-144.

Valizadeh, S., Rasoulifard, M.H. and Dorraji M.S.S. (2016), "Adsorption and photocatalytic degradation of organic dyes onto crystalline and amorphous hydroxyapatite: Optimization, kinetic and isotherm studies", *Korean J. Chem. Eng.*, **33**(2), 481-489.

Wei, W., Sun, R., Cui, J. and Wei, Z. (2010), "Removal of nitrobenzene from aqueous solution by adsorption on nanocrystalline hydroxyapatite", *Desalination*, **263**(1), 89-96.

Yang, Z., Fang, Z., Zheng, L., Cheng, W., Tsang, P.E., Fang, J. and Zha, D. (2016), "Remediation of lead contaminated soil by biochar-supported nano-hydroxyapatite", *Ecotox. Environ. Safe.*, **132**, 224-230.

Zhuang, F., Tan, R., Shen, W., Zhang, X., Xu, W. and Song, W. (2015), "Monodisperse magnetic hydroxyapatite/Fe3O4 microspheres for removal of lead(II) from aqueous solution", *J. Alloy. Compd.*, **637**, 531-537.

WL